Thermodynamic and transport properties of single-crystal $Yb_{14}MnSb_{11}$

I. R. Fisher, T. A. Wiener, S. L. Bud'ko, and P. C. Canfield
Ames Laboratory and Department of Physics and Astronomy, Iowa State University, Ames, Iowa 50011

J. Y. Chan* and S. M. Kauzlarich
Department of Chemistry, One Shields Avenue, University of California, Davis, California 95616
(Received 17 December 1998)

Relatively large (up to 250 mg) single crystals of the intermetallic compound $Yb_{14}MnSb_{11}$ have been prepared by a flux-growth technique. The results of thermodynamic and transport measurements of these samples are presented. The compound orders ferromagnetically at approximately $T_C = 53 \pm 1$ K, with a magnetization consistent with the assignment Mn^{3+} ($3d^4$) and Yb^{2+} ($4f^{14}$). The Mn moments are local in nature, with the full effective and saturated moment of the Hund's rule spin-only ground state. The electrical resistivity has a metallic temperature dependence, with only a modest anisotropy. Room-temperature values of the resistivity are relatively high for an intermetallic compound: $1630 \pm 160\ \mu\Omega$ cm and $1250 \pm 130\ \mu\Omega$ cm for currents flowing approximately parallel and perpendicular to the c axis, respectively. There is a distinct loss of spin-disorder scattering in the resistivity at T_C. From the heat capacity, a rough estimation of the magnetic entropy gives $\Delta S_M \approx 12.1$ J/mol K, the value in reasonable agreement with the expected $\Delta S_M \approx R \ln 5$ from the assignment of these moments. All of these data are consistent with a picture of Mn^{3+} local moments being coupled via conduction electrons. To this end, $Yb_{14}MnSb_{11}$ appears to be analogous to local-moment rare-earth intermetallic compounds, and may point the way toward a class of $3d$ Kondo lattice compounds. [S0163-1829(99)02021-4]

I. INTRODUCTION

The study of the magnetic properties of local $3d$ (Ti-Cu) moments in a metallic environment remains an active field of research. Depending on how the local $3d$ moments hybridize with the host conduction electrons, single-ion Kondo behavior is observed for some dilute magnetic alloys.[1,2] The virtual bound state has been a very useful concept in explaining this behavior.[3,4] Larger concentrations of the magnetic ions result in a stabilization of the local moment (typically for impurity concentrations >100 ppm), leading to a spin-glass ground state (see, for instance Mydosh[5]). In some ''dilute'' binary compounds, such as $MnAl_6$ and $MnZn_{13}$, $3d$ ''impurities'' are arranged on lattice sites, and coherent scattering from the virtual bound states can form a narrow hybrid band.[6–8] However, these systems have only modest γ values (the linear term in the specific-heat capacity at low temperatures, $\gamma = 62$ mJ/mol K^2), and, in the words of Coles, are barely ''slightly plump'' fermion systems.[9] In addition, the above ''dilute'' binary compounds exhibit only a fraction of the full moment expected from the spin-only Hund's rule ground state. In contrast, concentrated Kondo lattices with large γ values have been observed for several compounds containing $4f$ and $5f$ elements with a somewhat unstable f electron configuration.[9–12] Various ground states are experimentally observed, including long-range magnetic order [for instance, $CeAl_2$ (Ref. 12)], superconductivity [for instance, $CeCu_2Si_2$ (Ref. 13)], and possibly a nonmagnetic singlet [for instance, $CeAl_3$ (Ref. 9)]. It remains an open question as to whether a $3d$ intermetallic Kondo lattice can be achieved experimentally, with similarly large γ values to the $4f$ analogs.

In this paper, we present the thermodynamic and transport properties of a ternary compound $Yb_{14}MnSb_{11}$ in which all the magnetic properties arise from well-separated Mn ions (the Yb is divalent and hence nonmagnetic). This ''dilute'' $3d$ compound is significant because the Mn magnetism is local in character, and retains the full moment associated with the orbitally quenched Hund's rule ground state (i.e., the Mn does not seem to lose any of its magnetic nature to the conduction band). In this sense, $Yb_{14}MnSb_{11}$ is analogous to $4f$ intermetallic compounds. The ground state of this particular compound is a ferromagnetically ordered system, but this compound clearly points the way towards other dilute $3d$ compounds that may exhibit other, possibly novel, ground states.

The compound $Yb_{14}MnSb_{11}$ was synthesized by Chan *et al.* in 1998.[14] It is isostructural with the Zintl compound $Ca_{14}AlSb_{11}$,[15,16] crystallizing with a tetragonal lattice in the space group $I4_1/acd$. Other related compounds include $Eu_{14}MnSb_{11}$, which shows colossal magnetoresistance effects associated with a ferromagnetic transition coupled to a metal-insulator transition,[17–19] and $Eu_{14}MnBi_{11}$, which orders antiferromagnetically and shows a large negative magnetoresistance possibly associated with strong ferromagnetic fluctuations.[20] Extension of the Zintl concept to $Yb_{14}MnSb_{11}$ predicts that the Mn ions will be trivalent (i.e., a $3d^4$ configuration), while the Yb ions will be divalent ($4f^{14}$: i.e., nonmagnetic).[14] Initial magnetic measurements indicated a Curie-Weiss temperature dependence consistent with the theoretical valence assignment,[14] and a ferromagnetic transition temperature of approximately 56 K (although the saturated moment was ambiguous). The Mn ions are sufficiently far apart (≈ 10 Å) that they are unlikely to form an appreciable $3d$ band, and the exchange interaction between the Mn moments is most probably mediated by the conduction electrons [i.e., Ruderman-Kittel-Kasaya-Yosida exchange].[14] However, sample-purity issues prevented any firm conclusions from being drawn from these early measurements. Using

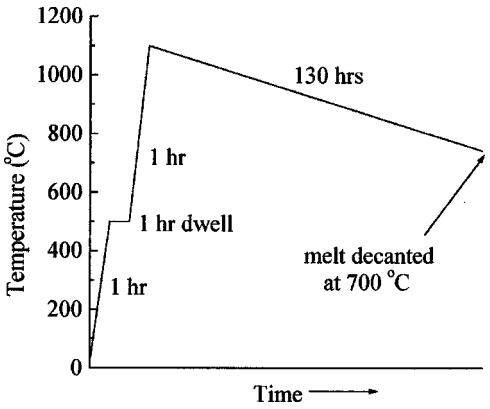

FIG. 1. A schematic diagram of the temperature profile used to grow single crystals of $Yb_{14}MnSb_{11}$ from a tin flux. Note that the time axis is not to scale.

flux-grown samples, which have a much higher purity and a much larger size than earlier polycrystalline samples and single crystals grown by vapor transport, we have been able to accurately confirm the valence assignment, and investigate the behavior of the Mn moments in much greater detail. Here we show the results of the measurements of the heat capacity through the ferromagnetic transition, and measurements of the anisotropic magnetization and electrical resistivity.

II. EXPERIMENTAL METHODS

Single crystals of $Yb_{14}MnSb_{11}$ were grown from a high-temperature solution, in a similar manner to CeSb as described by Canfield and Fisk.[21] Tin was chosen as a suitable flux, and an initial melt composition of $Yb_{14}Mn_6Sb_{11}Sn_{86}$ was found to produce the best-formed crystals. Elemental starting materials (Yb: Ames Laboratory 99.99%, Mn: Union Carbide 99.9%, Sb: Alfa Aesar 99.999%, Sn: 99.9%) were placed in a 5 ml alumina crucible, and sealed in a quartz glass ampoule with a small partial pressure of argon. The temperature profile used for the growth is shown schematically in Fig. 1 (note that the time axis is not to scale). The initial heating to 500 °C gently melts the tin flux, into which the remaining elements dissolve during the subsequent heating to 1100 °C. The crystals grow during the slow cooling (130 h), and the remaining melt is decanted at 700 °C. Crystals grown by this technique are relatively large (up to 250 mg), display a complex array of facets, and have morphologies that do not suggest any specific unit cell. This morphology is different from that of needlelike single crystals grown by reacting stoichiometric elements in sealed tantalum tubes in a two-zone furnace[14] (presumably this is some kind of a vapor transport crystal growth). However, powder x-ray-diffraction patterns show that both crystal growth methods produce the same compound, with second phases below the detection limit (approximately 5%). Magnetization measurements (see below) indicate much lower impurity levels in the flux-grown single crystals (this study) than in polycrystalline samples.[14]

Samples for anisotropic magnetization measurements were aligned relative to their crystallographic axes by Laue x-ray diffraction. The dc magnetization was measured along the principle axes [001] and [100] and along [110], using a commercial superconducting quantum interference device magnetometer. The magnetization as a function of temperature was measured in an applied field of 1 kOe for temperatures below the ferromagnetic transition, and 10 kOe for higher temperatures (up to 350 K). The magnetization as a function of applied field (up to 55 kOe) was measured at 5.0 K. Subsequently, the anisotropic magnetization was used to align bars relative to the crystallographic axes for transport measurements.

The bars for electrical resistivity measurements were cut and polished from the larger single crystals such that the final dimensions were approximately 2–3 mm in length with a cross section of approximately 0.6 mm×0.6 mm. The resistivity was measured by a standard four-probe technique, using an ac bridge operating at 16 Hz and with a current density of approximately 0.05 A cm^{-2}. Electrical contact was made to the samples using Epo-tek H20E silver epoxy, with typical contact resistances of 1–2 Ω. Uncertainty in the contact separation gives an estimated uncertainty of ±10% in the absolute value of the resistivity obtained. The estimated uncertainty in the orientation of the bars was ±15° for currents parallel (∥) to [001] and ±5° for currents perpendicular (⊥) to [001]. The bars with their length perpendicular to [001] were not aligned with respect to the [100] and [110] directions (these directions having the same magnetization).

The heat capacity of an approximately 20 mg single crystal of $Yb_{14}MnSb_{11}$ was measured from 2 to 100 K. The measurement was made using the heat-capacity option of a Quantum Design PPMS-9 instrument, utilizing the relaxation technique with fitting of the whole temperature response of the microcalorimeter. One side of the crystal was polished flat to ensure good thermal contact with the microcalorimeter.

III. RESULTS

A. dc magnetization

In the paramagnetic regime ($T>54$ K), the dc magnetic susceptibility of $Yb_{14}MnSb_{11}$ is isotropic (as expected for a spin-only $3d$ local moment with quenched orbital angular momentum), and can be fitted by a modified Curie-Weiss law:

$$\chi = \frac{C}{T-\theta} + \chi_0, \tag{1}$$

where C is the Curie constant, θ is the paramagnetic Curie temperature, and χ_0 is a small temperature-independent term. The susceptibility follows this temperature dependence [Eq. (1)] for all $T>T_C$. The small constant term χ_0 is the sum of contributions from core states and Pauli and Landau paramagnetism, and has a value of approximately $(1.29 \pm 0.01)\times 10^{-6}$ emu/g. The inset to Fig. 2(a) shows the inverse susceptibility $(\chi-\chi_0)^{-1}$ as a function of temperature. From C we find an effective moment (P_{eff}) per formula unit (f.u.) of $4.86\pm 0.02\mu_B$/f.u. (close to the calculated spin-only value of $4.9\mu_B$/Mn for local Mn^{3+} moments). The paramagnetic Curie temperature $\theta = 54.0\pm 0.1$ K, is very close to values for T_C estimated from the electrical resistivity (53.5 ±0.5 K) and the specific-heat capacity (51.8±0.3 K) (both discussed below). In general, to accurately estimate T_C from magnetization data requires detailed $M(H)$ measurements in the vicinity of the ferromagnetic transition. However, in this case, deviations from Eq. (1) are extremely small close to T_C

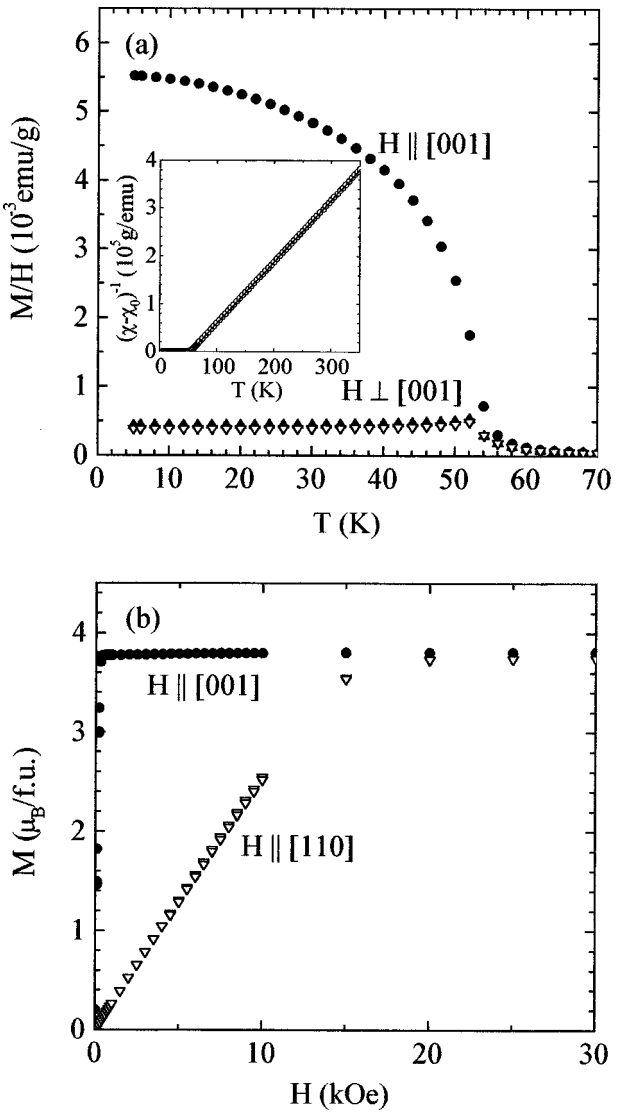

FIG. 2. Anisotropic magnetization of $Yb_{14}MnSb_{11}$ as a function of (a) temperature ($H=1$ kOe, zero-field-cooled) and (b) applied field ($T=5.0$ K). Solid circles $H\|[001]$, solid triangles $H\|[100]$, open triangles $H\|[110]$. Inset to panel (a) shows the inverse susceptibility $(\chi-\chi_0)^{-1}$ as a function of temperature in 10 kOe (symbols) and the fit to Eq. (1) (solid line indicates the fit parameters given in the main text). Panel (b) shows $M(H)$ data at $T=5.0$ K for both increasing and decreasing applied fields (which are essentially identical).

[see inset to Fig. 2(a)], and the measurement was made in a relatively low applied field, so the paramagnetic Curie temperature provides a relatively good estimate of the ferromagnetic transition temperature. This value (54.0 ± 0.1 K) is in good agreement with initial estimates from magnetic measurements of polycrystalline samples [56 K (Ref. 14)]. In addition, we note that the absence of large deviations from Curie-Weiss behavior close to T_C implies a good local-moment character (and absence of spin fluctuations) of the Mn spins.

For temperatures below T_C, the magnetization of $Yb_{14}MnSb_{11}$ is strongly anisotropic, with an easy axis along the c axis [001] [Fig. 2(a)]. The anisotropy is substantially more pronounced than for the needlelike single crystals grown previously,[14] presumably due to the less extreme geometric demagnetization effects of the flux-grown samples. The magnetization at 5.0 K [Fig. 2(b)] saturates rapidly for applied fields along the easy axis (M saturates at 300 Oe for $H\|[001]$, with a value of $3.81\mu_B$/Mn), but larger applied fields are necessary to fully saturate the moments for $H\perp[001]$ ($H>20\,000$ Oe for $H\|[110]$). The magnetization below T_C is reversible, indicating that these single-crystal samples are magnetically soft, consistent with there being little disorder for pinning of domain walls, and implying that zero-field-cooled and field-cooled magnetization data should agree in value (as observed).

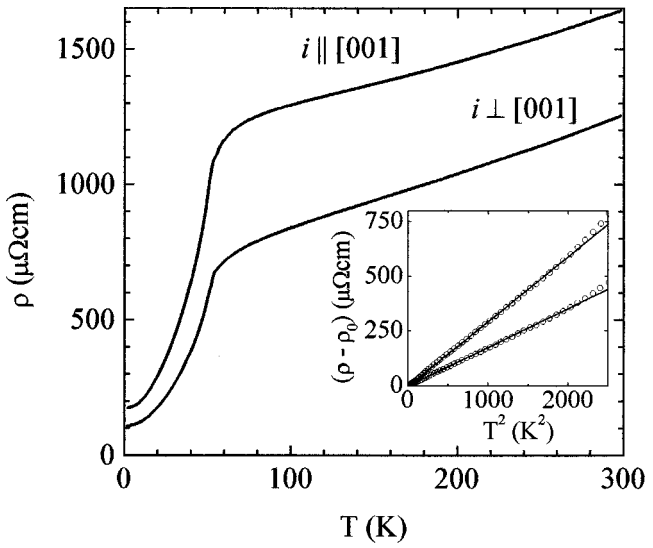

FIG. 3. Anisotropic resistivity of $Yb_{14}MnSb_{11}$. Current directions relative to the c axis [001] are shown in the figure. Inset shows $(\rho-\rho_0)$ vs T^2 for $T<T_C$, with linear fit to data shown by solid lines.

B. Resistivity and magnetoresistance

The electrical resistivity of $Yb_{14}MnSb_{11}$ is shown in Fig. 3, for currents (i) flowing approximately parallel and perpendicular to the c axis [001]. The orientations are not precise, but are within 15° ($i\|[001]$) and 5° ($i\perp[001]$) of the estimated orientations. The temperature dependence of the resistivity is metallic, with a significant loss of spin-disorder scattering at $T_C=53.5\pm0.5$ K (in agreement with values of T_C estimated from magnetization measurements). The sharp drop in the resistivity can be seen more clearly in Fig. 4. For $T<T_C$, the resistivity follows a T^2 temperature dependence, as expected for a ferromagnet (see inset to Fig. 3, showing the resistivity ρ less the residual resistivity ρ_0 vs T^2). The inclusion of second-order exponential terms does not significantly improve the linear fit shown in the inset to Fig. 3. The residual resistance ratio [we take $\rho(300\text{ K})/\rho(1.8\text{ K})$] is moderately large, having a value of 9.4 and 11.7 for currents flowing parallel and perpendicular to [001], respectively. There is a modest anisotropy in the resistivity (Fig. 3), with larger values for $i\|[001]$ than for $i\perp[001]$. The origin of this anisotropy is not immediately obvious, but is probably more related to the crystal and electronic structure than to the Mn magnetism (the magnetization being isotropic for $T>T_C$). Room-temperature values of the resistivity are relatively high for an intermetallic compound: $1630\pm160\,\mu\Omega$ cm and $1250\pm130\,\mu\Omega$ cm for currents flowing parallel and perpen-

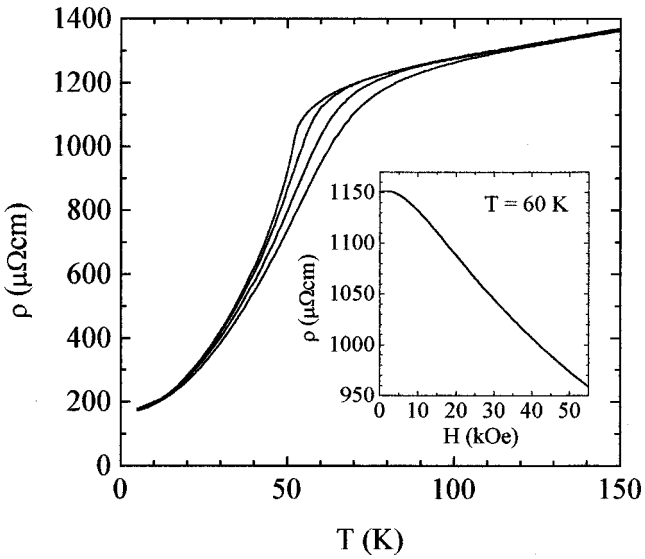

FIG. 4. The resistivity of $Yb_{14}MnSb_{11}$ for currents flowing parallel to [001] in applied magnetic fields of 0, 10, 30, and 55 kOe ($H \| [001]$). Larger magnetic fields increase T_C. The inset shows the resistivity as a function of applied field at $T = 60$ K.

dicular to the *c*-axis respectively, suggesting that $Yb_{14}MnSb_{11}$ may have a relatively low carrier concentration.

The effect of magnetic fields on the electrical resistivity close to the ferromagnetic transition is shown in Fig. 4. The longitudinal magnetoresistance was measured for the current orientation $i \| [001]$ and for applied fields also parallel to [001]. As can be seen in Fig. 4, applied fields broaden the loss of spin-disorder scattering associated with the onset of long-range magnetic order. The magnetoresistance was followed as a function of applied field at $T = 60$ K (i.e., a temperature just greater than T_C), and is shown in the inset to Fig. 4. The negative magnetoresistance is caused by the reduction in spin-disorder scattering as the Mn moments partially align in the applied field. This effect is much smaller than has recently been observed for the isostructural compound $Eu_{14}MnBi_{11}$ which orders antiferromagnetically at $T_N = 32$ K (despite predominantly ferromagnetic Mn-Mn exchange).[20] In that case, a substantial negative magnetoresistance for $T > T_N$ was interpreted as possible evidence for strong ferromagnetic fluctuations, in addition to a reduction of spin-disorder scattering. Also, a larger magnetoresistance than we find for $Yb_{14}MnSb_{11}$ was observed for the isostructural ferromagnetic compound $Eu_{14}MnSb_{11}$,[19] although in that case the resistivity is nonmetallic (weakly semiconducting) for $T > T_C$, and apparently metallic for $T < T_C$.

C. Heat capacity

The molar heat capacity of $Yb_{14}MnSb_{11}$ from 2 to 100 K is shown in Fig. 5. The well-defined peak at $T = 51.8 \pm 0.3$ K marks the ferromagnetic ordering transition. The ordering temperature is consistent with the magnetization and resistivity results discussed above. Low-temperature heat capacity can be fitted taking into account electronic ($C_e \propto T$), lattice ($C_{\text{lat}} \propto T^3$), and magnetic spin waves in an anisotropic ferromagnet [$C_M \propto T^{3/2} \exp(-\Delta/T)$] contributions. This fit yields the electronic specific-heat coefficient $\gamma \approx 45 \pm 20$ mJ/mol K^2 and the value of the gap in the magnon spectrum $\Delta \approx 13$ K. As shown in Fig. 6, a linear fit to C/T vs T^2 at the very lowest temperatures (from 2 to 7 K) yields an estimate of $\gamma \approx 70 \pm 20$ mJ/mol K^2. This value is similar to that found for the isostructural compounds $Sr_{14}MnBi_{11}$ and $Ba_{14}MnBi_{11}$ (approximately 100 mJ/mol K^2).[22] The Debye temperature Θ_D, estimated for $T > T_C$, is 160 ± 10 K.

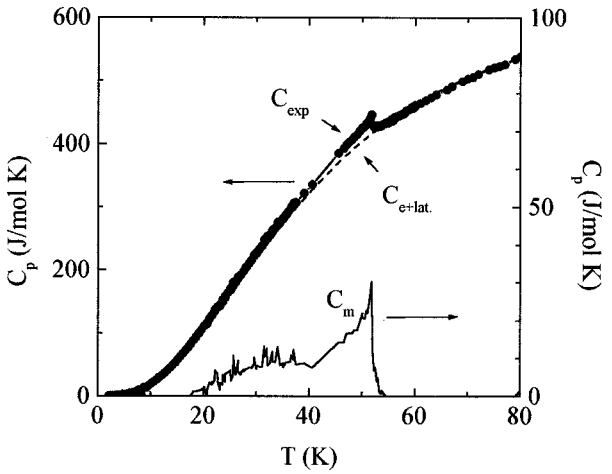

FIG. 5. The molar heat capacity of $Yb_{14}MnSb_{11}$. Experimental data are indicated by C_{exp}, while estimates of the magnetic, electronic, and lattice components are indicated by C_m and $C_{e+\text{lat}}$ (see main text).

Due to the complex low-temperature behavior of the specific heat and limited range of the measurements, the calculation of the magnetic entropy associated with the ferromagnetic ordering transition in $Yb_{14}MnSb_{11}$ is somewhat ambiguous. Nevertheless if we approximate the ''background'' contribution to the specific heat as a smooth interpolation between low-temperature and high-temperature (well above the transition) data (Fig. 5), the rough estimation of the magnetic entropy

$$\Delta S_M = \int (C_M/T)\,dT \tag{2}$$

will give $\Delta S_M \approx 12.1$ J/mol K$\approx 1.46R$, the value in reasonable agreement (91%) with the expected $\Delta S_M \approx R \ln 5$.

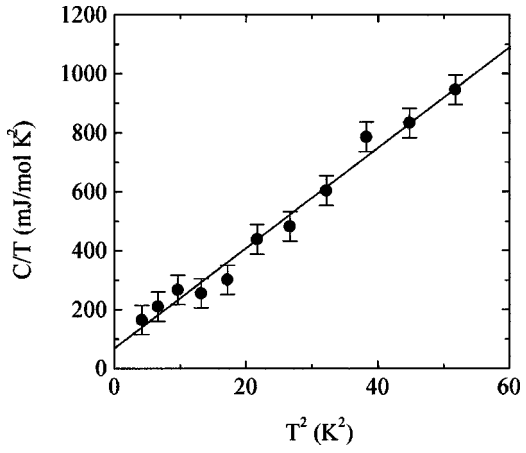

FIG. 6. C/T vs T^2 for $Yb_{14}MnSb_{11}$, for temperatures from 2 to 7 K. The line shows linear fit to these data.

IV. DISCUSSION

Estimates of the magnetic ordering temperature of $Yb_{14}MnSb_{11}$ from all measurements agree well. Comparing estimates from the susceptibility (54.0 ± 0.1 K), the electrical resistivity (53.5 ± 0.5 K), and the heat capacity (51.8 ± 0.3 K) we arrive at a combined estimate of 53 ± 1 K (the uncertainty here represents the differences in T_C obtained from the different measurements).

The observed effective moment of $Yb_{14}MnSb_{11}$ ($4.86 \pm 0.02 \mu_B$/Mn) is very close to the spin-only value expected for trivalent Mn ($4.9 \mu_B$/Mn). The compound $Yb_{14}MnSb_{11}$ has 8 formula units per unit cell, with only one Mn site, but four different 2+ cation (Yb) sites.[14,15] The Yb site with the minimum multiplicity corresponds to 2 Yb ions per formula unit, which if trivalent would result in an effective moment significantly larger than that which is observed. In addition, Yb^{3+} would result in an anisotropic magnetization for $T > T_C$ due to crystal electric-field splitting of the Yb Hund's rule J multiplet, which we do not observe. It follows that the observed value of P_{eff} is good evidence that all of the Mn ions are in the Mn^{3+} state (a $3d^4$ configuration), while all Yb ions are divalent (nonmagnetic), consistent with previous measurements of polycrystalline material.[14] In addition, the observed saturated moment of $3.81 \pm 0.01 \mu_B$/Mn is close to the expected value of $4 \mu_B$/Mn for four unpaired electrons, consistent with the above valence arrangement. Since the saturation magnetization is the same for all field orientations [Fig. 2(b)], the small difference between the observed value of the saturated moment and that expected for Mn^{3+} is unlikely to be due to sample misorientations, and may hint at a small bandlike component to the ferromagnetism. However, the temperature dependence of the susceptibility [inset to Fig. 2(a)] suggests that the Mn ions are behaving as truly local moments. In addition, we note that the saturation moment obtained for polycrystalline samples is substantially larger than $4 \mu_B$/f.u. [up to $6.6 \mu_B$/f.u. (Ref. 14)], implying the presence of magnetic second phases in the polycrystalline samples. The data for these single crystals has therefore significantly clarified the valence assignments. The observation of a magnetic entropy close to $R \ln 5$ adds further weight to the suggested valence assignments.

Having established that the observed magnetic behavior originates from local Mn moments, it is instructive to make the comparison of the physical properties of $Yb_{14}MnSb_{11}$ with those of a previously discussed ''dilute'' $3d$ compound, $MnZn_{13}$.[6,7] In the case of $MnZn_{13}$, a local moment is inferred from the Curie-Weiss temperature dependence of the magnetic susceptibility. However, significant deviations from this temperature dependence are observed below 120 K, suggesting the importance of strong Mn-Mn interactions well above $T_C = 23$ K, perhaps due to the anisotropic crystal structure (Mn-Mn distances are closer along chains in the c-axis direction, but these chains cannot support long-range order until the interchain interaction is strong enough). The observed effective moment of $MnZn_{13}$ (for temperatures greater than the above deviations) is only $1.8 \mu_B$/Mn, substantially less than that expected from the spin-only Hund's rule ground state of either Mn^{3+} or Mn^{4+}. In addition, the saturated moment is only $0.3 \mu_B$/Mn. In contrast, in the mixed compound $Mn_{0.05}Fe_{0.95}Zn_{13}$ the Mn carries the full moment of $4 \mu_B$/Mn (Fe is nonmagnetic). In this sense, $MnZn_{13}$ is not the ideal dilute $3d$ compound to study. In contrast, $Yb_{14}MnSb_{11}$ is a much better dilute $3d$ compound, with a significantly larger Mn-Mn distance of approximately 10 Å (the Mn-Mn distance of $MnZn_{13}$ is 6.6 Å). Both the effective and saturated moments of $Yb_{14}MnSb_{11}$ are consistent with the full moment of Mn^{3+}, and the susceptibility follows a Curie-Weiss temperature dependence for all temperatures greater than T_C. The reason for the good local moment character is not clear, but may be associated with a low carrier density around the Mn ions. In addition, the $3d$ level is probably significantly below the Fermi energy. In this sense, $Yb_{14}MnSb_{11}$ is a direct analog of $4f$ intermetallic systems, despite the differences in the $3d$ and $4f$ orbital radii relative to that of the free ions. The linear term in the specific-heat capacity of both compounds is similar (around 60 mJ/mol K^2), and is far from being deemed that of a heavy fermion. However, this compound is clearly a step towards the goal of finding a $3d$ intermetallic equivalent of the $4f$ Kondo lattices discussed earlier.

V. CONCLUSIONS

The results presented in this paper have clarified and extended the initial work of Chan *et al.*[14] on polycrystalline samples of $Yb_{14}MnSb_{11}$. This intermetallic compound orders ferromagnetically at 53 K. The magnetic behavior is consistent with a picture of local Mn^{3+} moments, in a metallic environment. In this sense, $Yb_{14}MnSb_{11}$ is analogous to magnetic rare-earth ($4f$) containing compounds, and is a particularly good example of a ''dilute'' $3d$ compound. In spite of the relatively high ferromagnetic ordering temperature, it remains an interesting question as to whether hybridization effects can be observed for lower Mn concentrations (for instance by considering dilutions such as $Yb_{14}Al_{1-x}Mn_xSb_{11}$). Experiments are currently in progress to investigate this possibility. If Kondo-like behavior can be observed in such a system, then this might suggest that similar intermetallic compounds (possibly related to other Zintl phases) are the best starting place in the search for a $3d$ intermetallic Kondo lattice. The principle features of this system are relatively dilute local $3d$ moments in a metallic environment with a fairly low carrier concentration. The advantage of looking at ternary compounds is principally one of tunability (more free parameters to adjust via substitutions and choice of element), but also the larger number of possible compounds of a ternary over a binary system.

ACKNOWLEDGMENTS

We are grateful to Z. Islam for aligning samples for magnetization measurements by Laue x-ray diffraction. J.Y.C. and S.M.K. were supported by the NSF (DMR-9505565). Ames Laboratory is operated for the US Department of Energy under Contract No. W-7405-Eng-82. This work was supported by the Director for Energy Research, Office of Basic Energy Sciences.

*Present address: Materials Science and Engineering Laboratory, NIST, Ceramics Division, Bldg. 223-A256, Gaithersburg, MD 20899.

[1] A. J. Heeger, in *Solid State Physics*, edited by F. Seitz, D. Turnbull, and H. Ehrenreich (Academic, New York, 1969), Vol. 23, p. 283.
[2] G. Gruner, Adv. Phys. **23**, 941 (1974).
[3] J. Friedel, Can. J. Phys. **34**, 1190 (1956).
[4] P. W. Anderson, Phys. Rev. **124**, 41 (1961).
[5] J. A. Mydosh, *Spin Glasses: An Experimental Introduction* (Taylor and Francis, London, 1993).
[6] A. D. Caplin, J. B. Dunlop, and R. H. Taylor, J. Phys. (Paris), Colloq. **32**, C1-209 (1971).
[7] A. D. Caplin and J. B. Dunlop, J. Phys. F **3**, 1621 (1973).
[8] G. Gruner and N. F. Mott, J. Phys. F **4**, L16 (1974).
[9] B. R. Coles, Contemp. Phys. **28**, 143 (1987), and references therein.
[10] G. R. Stewart, Rev. Mod. Phys. **56**, 755 (1984), and references therein.
[11] Z. Fisk, H. R. Ott, T. M. Rice, and J. L. Smith, Nature (London) **320**, 124 (1986), and references therein.
[12] H. R. Ott, Prog. Low Temp. Phys. **11**, 216 (1987), and references therein.
[13] F. Steglich, C. D. Bredl, W. Lieke, U. Rauchschwalbe, and G. Sparn, Physica B **126**, 82 (1984).
[14] J. Y. Chan, M. M. Olmstead, S. M. Kauzlarich, and D. J. Webb, Chem. Mater. **10**, 3583 (1998).
[15] G. Cordier, H. Schäfer, and M. Stelter, Z. Anorg. Allg. Chem. **519**, 183 (1984).
[16] S. M. Kauzlarich, in *Chemistry, Structure and Bonding of Zintl Phases and Ions*, edited by S. M. Kauzlarich (VCH, New York, 1996), p. 245.
[17] A. Rehr and S. M. Kauzlarich, J. Alloys Compd. **207&208**, 424 (1994).
[18] J. Y. Chan, M. E. Wang, A. Rehr, S. M. Kauzlarich, and D. J. Webb, Chem. Mater. **9**, 2131 (1997).
[19] J. Y. Chan, S. M. Kauzlarich, P. Klavins, R. N. Shelton, and D. J. Webb, Chem. Mater. **9**, 3132 (1997).
[20] J. Y. Chan, S. M. Kauzlarich, P. Klavins, R. N. Shelton, and D. J. Webb, Phys. Rev. B **57**, 8103 (1998).
[21] P. C. Canfield and Z. Fisk, Philos. Mag. B **65**, 1117 (1992).
[22] D. P. Siemens, J. Del Castillo, W. Potter, D. J. Webb, T. Y. Kuromoto, and S. M. Kauzlarich, Solid State Commun. **84**, 1029 (1992).